Planta (2020) 251:95
https://doi.org/10.1007/s00425-020-03383-5

ORIGINAL ARTICLE

Carotenogenesis and chromoplast development during ripening of yellow, orange and red colored *Physalis* fruit

Xin Wen[1,2,3] · Annerose Heller[4] · Kunli Wang[1] · Qianyun Han[1] · Yuanying Ni[1] · Reinhold Carle[2,5] · Ralf Schweiggert[2,6]

Received: 30 October 2019 / Accepted: 25 March 2020 / Published online: 9 April 2020

Abstract

Main conclusion **Formation of specific ultrastructural chromoplastidal elements during ripening of fruits of three different colored *Physalis* spp. is closely related to their distinct carotenoid profiles.**

Abstract The accumulation of color-determining carotenoids within the chromoplasts of ripening yellow, orange, and red fruit of *Physalis pubescens* L., *Physalis peruviana* L., and *Physalis alkekengi* L., respectively, was monitored by high-performance liquid chromatography/diode array detector/tandem mass spectrometry (HPLC–DAD-MS/MS) as well as light and transmission electron microscopy. Both yellow and orange fruit gradually accumulated mainly β-carotene and lutein esters at variable levels, explaining their different colors at full ripeness. Upon commencing β-carotene biosynthesis, large crystals appeared in their chromoplasts, while large filaments protruding from plastoglobules were characteristic elements of chromoplasts of orange fruit. In contrast to yellow and orange fruit, fully ripe red fruit contained almost no β-carotene, but esters of both β-cryptoxanthin and zeaxanthin at very high levels. Tubule bundles and unusual disc-like crystallites were predominant carotenoid-bearing elements in red fruit. Our study supports the earlier hypothesis that the predominant carotenoid type might shape the ultrastructural carotenoid deposition form, which is considered important for color, stability and bioavailability of the contained carotenoids.

Keywords Carotenoids · Deposition · Ultrastructure · Xanthophyll esters · Tubules · Disc-like crystallites

Abbreviations

RS Ripening stage
TSS Total soluble solids
TEM Transmission electron microscopy

Introduction

Carotenoids are naturally occurring hydrophobic compounds, often imparting yellow, orange, and red colors to numerous fruits, vegetables, and flowers. Besides their biological functions in plants, e.g., supporting light harvest for photosynthesis, carotenoids play an important role in the color of plant foods, being vital for the economic value of the respective produce (Nisar et al. 2015). In addition, the dietary consumption of carotenoid-rich foods has been

Electronic supplementary material The online version of this article (https://doi.org/10.1007/s00425-020-03383-5) contains supplementary material, which is available to authorized users.

✉ Yuanying Ni
niyycau@hotmail.com; nyy@cau.edu.cn

[1] College of Food Science and Nutritional Engineering, National Engineering Research Center for Fruit and Vegetable Processing, Key Laboratory of Fruit and Vegetable Processing, Ministry of Agriculture, China Agricultural University, Beijing 100083, China

[2] Chair of Plant Foodstuff Technology and Analysis, Institute of Food Science and Biotechnology, University of Hohenheim, 70599 Stuttgart, Germany

[3] College of Resources and Environmental Sciences, National Academy of Agriculture Green Development, China Agricultural University, Beijing 100193, China

[4] Institute of Botany, University of Hohenheim, 70599 Stuttgart, Germany

[5] Biological Science Department, King Abdulaziz University, P. O. Box 80257, Jeddah 21589, Saudi Arabia

[6] Chair of Analysis and Technology of Plant-Based Foods, Institute of Beverage Research, Geisenheim University, 65366 Geisenheim, Germany

associated with numerous health-promoting effects in humans. The most prominent benefit is that some derivatives serve as precursors of vitamin A, such as α- and β-carotene as well as β-cryptoxanthin. Vitamin A is important for the visual system, immune function, as well as normal growth and development (Grune et al. 2010). Beyond vitamin A supply, growing evidence suggests an important role of the oxygenated carotenoids lutein and zeaxanthin in visual performance as well as protection and prevention against chronic eye-related diseases such as age-related macular degeneration (AMD) and retinitis pigmentosa. Both lutein and zeaxanthin, the so called "macular pigments", are selectively accumulated in the *macula lutea* at comparably high concentrations, strongly suggesting a biological function within the retina (Bernstein et al. 2016). Additionally, their potential role in maintaining cognitive health throughout the lifespan has been gradually recognized in recent years (Johnson 2014).

A rich source of provitamin A carotenoids as well as of lutein and zeaxanthin are the fruit of *Physalis* spp. The genus *Physalis* belongs to the Solanaceae family comprising several herbaceous plant species, among them including *P. alkekengi*, *P. pubescens*, and *P. peruviana*. Their fruit are becoming increasingly popular worldwide, offering great economic potential due to their expanding intensive cultivation and good storability during shipping (Etzbach et al. 2018). In addition, they have been reported to contain several health-promoting constituents (Bravo et al. 2015; Olivares-Tenorio et al. 2016; Wen et al. 2017, 2019; Etzbach et al. 2018). *Physalis* fruit display varying colors from green to red and sometimes purple among various species (Whitson and Manos 2005), which are attributed to the high concentration of chlorophylls, carotenoids, or anthocyanins. Our previous study highlighted the red colored *Physalis* (*Physalis alkekengi*) fruit as rich sources of dietary zeaxanthin and provitamin A-active β-cryptoxanthin, while yellow colored *Physalis* (*P. pubescens*) fruit contained mainly β-carotene and lutein (Wen et al. 2017). Etzbach et al. (2018) identified the carotenoid profile of orange colored *Physalis* fruit (gooseberry, *P. peruviana*) to be dominated by β-carotene and lutein esters. However, whether the abundant amounts of carotenoids in fruit of these three *Physalis* species are highly or poorly bioavailable remains to be elucidated, since liberation and absorption of carotenoids from plant matrix has been shown to be highly variable.

Among various factors influencing bioavailability of carotenoids, their genuine deposition forms within the chromoplasts, including lipid-dissolved forms in plastoglobules, liquid-crystalline forms in tubules, protein-bound forms in membranes, and solid-crystalline forms in crystalloids, represent an inherent highly decisive factor (Sitte et al. 1980; Schweiggert and Carle 2017). In the meantime, an increasing number of studies suggest that the development of these substructures may be widely driven by a self-assembly process and, thus, closely related to the molecular structure of the major carotenoid deposited (Vásquez-Caicedo et al. 2006; Montefiori et al. 2009; Schweiggert et al. 2011a; Fu et al. 2012; Jeffery et al. 2012; Kilcrease et al. 2015; Lado et al. 2015; Chacón-Ordóñez et al. 2016; Schweiggert and Carle 2017; Hempel et al. 2017; Rojas-Garbanzo et al. 2017; Berry et al. 2019; Huang et al. 2019), although the clear relationship is still not well understood. The comparative study of carotenoid profile and chromoplast substructures within the same genus or species has provided valuable insights, but has been only conducted in a few fruits and vegetables, e.g., in papaya (Schweiggert et al. 2011a), *Citrus* fruit (Lado et al. 2015), and *Capsicum annum* fruit (Kilcrease et al. 2015; Berry et al. 2019). Due to their interestingly different carotenoid profiles comprising carotenes, xanthophylls and/or xanthophyll esters, we sought to elucidate the development of chromoplasts and carotenoid profiles during ripening of three different colored *Physalis* fruit to provide further insights into the relationship between carotenoid composition and deposition form.

Materials and methods

Plant material and reagents

Fresh fruit of three different *Physalis* species with yellow (*P. pubescens*), orange (*P. peruviana*) and red (*P. alkekengi*) color were obtained at three ripening stages (RS1, RS2 and RS3, cf. Suppl. Figs. S1, S2, S3) from the Botanical Garden of the University of Hohenheim (Stuttgart, Germany) from June to September of 2017. A total of 30 fruit were harvest at each ripening stage for each species. All reagents were of analytical or HPLC grade. Ultrapure water was used throughout.

Carotenoid analyses

After careful removal of the calyces, the edible mesocarp (pulp) and exocarp (peel) of *Physalis* fruit were separated manually and cut into small (ca. 0.5–1.0 cm^3 and 1 cm^2, resp.) sections. Seeds were not separated from the pulp. After grinding the sections with mortar and pestle, an aliquot of 2.0 g of freshly ground mesocarp was extracted with a ternary mixture (1:1:1, v/v/v) of methanol, ethyl acetate and light petroleum (b.p. 40–60 °C), containing each 0.1 g/L of butylated hydroxytoluene and butylated hydroxyanisole, as described by Schweiggert et al. (2011b), where also further details may be found. Exocarp sections were extracted using the method of Chacón-Ordóñez et al. (2016) with slight modifications. Briefly, an aliquot of 200 mg freshly ground exocarp sections were soaked for 1 h in 3 mL acetone and

then extracted using a Sonopuls HD 3100 probe-sonicator (Bandelin, Berlin, Germany) equipped with a MS 72 probe at 70% amplitude for 30 s. After centrifugation (1315 × *g*, 3 min), the supernatant was collected and the solid remainders were re-extracted 3–4 times until being colorless. The collected supernatants were combined and phase-separated by adding hexane. All organic extracts were dried under a gentle stream of nitrogen and stored at − 80 °C until HPLC analyses.

Prior to HPLC–DAD–MS/MS analyses, the dried extracts were dissolved in a mixture of *tert*-butyl methyl ether and methanol (1:1, v/v) and membrane-filtered (0.45 µm, Polytetrafluoroethylene (PTFE), Chromafil, Macherey–Nagel, Düren, Germany) into amber HPLC vials.

Identification and quantification of carotenoids was conducted by the two methods described for yellow and red *Physalis* fruits by Wen et al. (2017). Carotenoid analyses of samples from orange *Physalis* were performed using the procedure for yellow *Physalis*. Identification of (all-*E*)-violaxanthin, (all-*E*)-neoxanthin, (all-*E*)-lutein, (all-*E*)-zeaxanthin, (all-*E*)-β-cryptoxanthin, (all-*E*)-α-carotene, and (all-*E*)-β-carotene was verified by comparing retention times, UV/Vis absorption and mass spectra to those of authentic standards (CaroteNature, Ostermundigen, Switzerland). Compounds for which standards were unavailable were identified by comparing their UV/Vis absorption and mass spectra with previously published data (Britton 1995; Breithaupt et al. 2002; Zanatta and Mercadante 2007; De Rosso and Mercadante 2007; Dugo et al. 2008; Van Breemen et al. 2012; Melendez-Martinez et al. 2013; Hempel et al. 2014, 2017; Rivera et al. 2014; Delgado-Pelayo et al. 2014, 2016; Ziegler et al. 2015; Facundo et al. 2015; Gupta et al. 2015; Petry and Mercadante 2016; Schweiggert et al. 2016; Turcsi et al. 2016; Mercadante et al. 2017; Wen et al. 2017; Chacón-Ordóñez et al. 2017; Etzbach et al. 2018). For the identification of β-carotene (*Z*)-isomers, D_B/D_{II} ratios were determined according to Britton (1995) and compared to literature data (Melendez-Martinez et al. 2013). Free carotenoids were quantitated by linear external calibration of authentic standards, while their corresponding esters were determined using the calibration of the corresponding free carotenoids applying respective molecular weight correction factors. Relative carotenoid concentrations were calculated by dividing the absolute concentration of the individual carotenoid by the total carotenoid content and multiplying with 100%.

Microscopy

For light microscopy, fresh fruit were cut into halves and freehand sections were taken from the exocarp (peel) and the adjacent mesocarp (Fig. 1) using razor blades. An Axioplan microscope (Zeiss, Oberkochen, Germany) coupled to a digital camera (Leica DMC 2900, Leica, Wetzlar, Germany) was used to characterize chloroplast and chromoplast development in bright field. Lugol's iodine solution was used to examine the presence of starch granules during chromoplast development.

For Transmission electron microscopy (TEM), small sections of meso- and exocarp (ca. 0.5 × 1.0 × 2.0 mm^3) were prepared using razor blades and immediately fixed in buffered 3% glutaraldehyde solution (0.1 M sodium phosphate buffer, pH 7.2) for 90 min, then washed three times for 10 min in buffer (see above). Subsequently, the samples were post-fixed in buffered 1% osmium tetroxide solution for 2 h and washed three times for 10 min with ultrapure water. For dehydration, the progressive-lowering-of-temperature method was applied (1 h in 30% ethanol at 0 °C, 1 h in 50% ethanol at − 20 °C, overnight in 70% ethanol at − 35 °C, 1 h in 90% ethanol at − 35 °C, and 1 h in 100% ethanol at − 35 °C). After warming to room temperature, samples were infiltrated and embedded in LR-White resin (Science

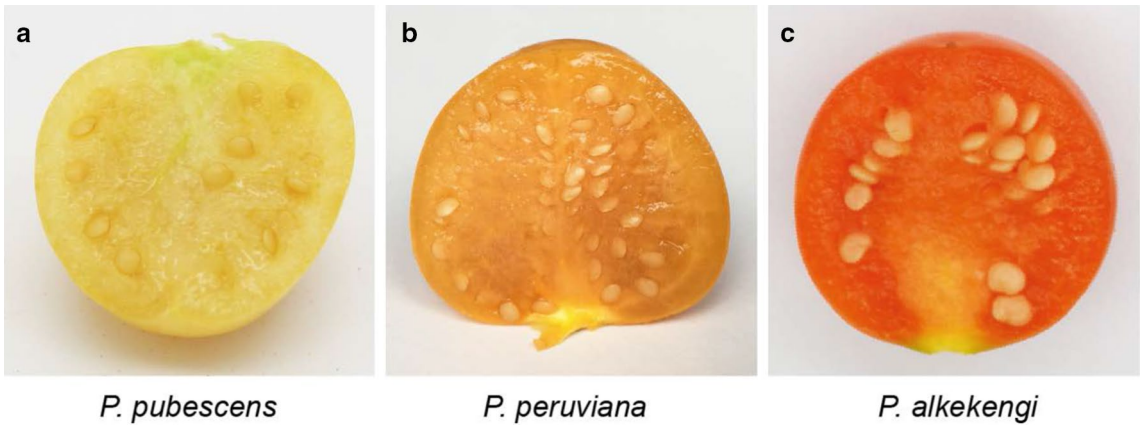

Fig. 1 Photographs of longitudinal sections of fruit at full ripeness. **a** *P. pubes*cens (yellow). **b** *P. peruviana* (orange). **c** *P. alkekengi* (red)

Service, Munich, Germany), and then polymerized at 60 °C for 24 h. Ultrathin sections were obtained using an Ultracut UCT ultratome (Leica, Wetzlar, Germany) equipped with a diamond knife (Drukker, Cuijk, Netherlands) and then collected on Pioloform and carbon-coated copper grids. Prior to investigation in an EM 10 transmission electron microscope (Zeiss, Oberkochen, Germany) at 60 kV, the ultrathin sections were stained with uranyl acetate and lead citrate. For documentation, the Megaview II (Soft Imaging System, Münster, Germany) and the analog camera of the EM10 were used. TEM negatives were digitalized with an Epson Perfection 2450 scanner. Photoshop CS6 (Adobe Systems, San José, CA, USA) was used to adjust contrast and brightness if necessary.

Statistics

All carotenoid extractions were performed in duplicate on two pooled batches of each 12 fruit. Data were reported as mean ± standard deviations (SD). One-way analyses of variance (ANOVA) with Tukey's honestly significant difference (HSD) post hoc test were conducted to determine significant differences between means ($P < 0.05$). All statistical analyses were carried out using SPSS version 20.0 (SPSS Inc., Chicago, IL, USA).

Results

Changes in carotenoid profiles of different colored *Physalis* fruit during maturation

Physalis fruit of all studied species (*P. alkekengi, P. peruviana, P. pubescens*) were green colored at the unripe stage RS1 as shown in Suppl. Fig. S1, S2, S3. At the early ripening stage (RS1), the total soluble solids (TSS) of yellow, orange and red *Physalis* fruit were about 10.0, 10.5 and 8.5 Brix, respectively, then increased to about 12.8, 13.2 and 10.8 Brix at the "color-break" stage (RS2), respectively. At full ripeness (RS3), yellow, orange and red *Physalis* fruit were characterized by TSS of about 13.2, 14.1 and 12.2 Brix, respectively. The corresponding carotenoid profiles and their changes during subsequent maturation in both mesocarp (pulp) and exocarp (peel) of *Physalis* fruit are shown in Tables 1, 2 and 3. At RS1, total carotenoid contents were found to be lower in pulp (0.33, 0.81, 1.44 mg/100 g FW) than in peel (6.96, 4.71, 10.86 mg/100 g FW) of yellow, orange and red *Physalis* types, respectively.

Among non-esterified carotenoids at RS1, (all-*E*)-lutein, (all-*E*)-β-carotene and (*Z*)-isomers of β-carotene were predominant in all *Physalis* fruit at RS1, accounting for proximately 31.6–76.2% of total carotenoids in pulp or 44.6–94.2% in peel. Further non-esterified carotenoids were

Table 1 Carotenoid composition of yellow *Physalis* (*P. pubescens*) fruit (meso- and exocarp) at different ripening stages

Compounds	Carotenoid content (mg/100 g FW)					
	Pulp			Peel		
	RS1	RS2	RS3	RS1	RS2	RS3
(all-*E*)-violaxanthin	tr	tr	tr	tr	tr	tr
(all-*E*)-neoxanthin	tr	tr	tr	tr	tr	tr
(all-*E*)-lutein	0.18 ± 0.00a	0.12 ± 0.00b	0.03 ± 0.00c	5.46 ± 0.21A	2.19 ± 0.64B	0.37 ± 0.17C
(15*Z*)-β-carotene	tr	tr	tr	0.02 ± 0.00A	0.03 ± 0.00AB	0.08 ± 0.02B
(13*Z*)-β-carotene	tr	tr	0.01 ± 0.00	tr	tr	0.42 ± 0.14
(all-*E*)-α-carotene	tr	tr	tr	tr	tr	0.05 ± 0.01
(all-*E*)-β-carotene	0.06 ± 0.00a	0.11 ± 0.00b	0.24 ± 0.02c	0.93 ± 0.07A	1.83 ± 0.31A	4.07 ± 0.58B
(9*Z*)-β-carotene	0.01 ± 0.00a	0.01 ± 0.00b	0.01 ± 0.00a	0.15 ± 0.01A	0.28 ± 0.05AB	0.33 ± 0.03B
Lutein dimyristate	0.05 ± 0.00a	0.08 ± 0.00b	0.06 ± 0.00c	0.27 ± 0.07A	0.73 ± 0.13B	0.93 ± 0.01B
Lutein 3-*O*-myristate-3′-*O*-palmitate	0.01 ± 0.00a	0.02 ± 0.00b	0.01 ± 0.00a	0.04 ± 0.01A	0.15 ± 0.01B	0.12 ± 0.02B
Lutein 3-*O*-palmitate-3′-*O*-myristate	0.01 ± 0.00a	0.03 ± 0.00b	0.02 ± 0.00ab	0.08 ± 0.01A	0.26 ± 0.02B	0.25 ± 0.03B
Lutein dipalmitate	0.01 ± 0.00a	0.01 ± 0.00b	0.01 ± 0.00c	0.02 ± 0.00A	0.08 ± 0.01B	0.05 ± 0.01C
Total free carotenoids	0.25 ± 0.00a	0.24 ± 0.00a	0.30 ± 0.02b	6.55 ± 0.29A	4.33 ± 1.00A	5.31 ± 0.55A
Total carotenoid esters	0.08 ± 0.00a	0.15 ± 0.00b	0.11 ± 0.00c	0.40 ± 0.08A	1.22 ± 0.13B	1.35 ± 0.01B
Total carotenoids	0.33 ± 0.00a	0.39 ± 0.01b	0.41 ± 0.02b	6.96 ± 0.38A	5.55 ± 1.13A	6.66 ± 0.54A

RS ripening stage, *tr* not quantified trace amount ($S/N < 10$)

Data represent mean values ± standard deviation ($n = 2$), different lowercase letters within a row indicate significant differences of carotenoid contents in pulp of yellow *Physalis* fruit ($P < 0.05$), different uppercase letters within a row indicate significant differences of carotenoid contents in peel of yellow *Physalis* fruit ($P < 0.05$)

Table 2 Carotenoid composition of orange *Physalis* (*P. peruviana*) fruit (meso- and exocarp) at different ripening stages

Compounds	Carotenoid content (mg/100 g FW)					
	Pulp			Peel		
	RS1	RS2	RS3	RS1	RS2	RS3
(all-*E*)-violaxanthin	tr	tr	tr	tr	tr	tr
(all-*E*)-neoxanthin	tr	tr	tr	tr	tr	tr
(all-*E*)-lutein	0.11 ± 0.01a	0.13 ± 0.00b	0.14 ± 0.00b	2.16 ± 0.59A	1.35 ± 0.15A	1.78 ± 0.01A
(15*Z*)-β-carotene	tr	0.01 ± 0.00	0.01 ± 0.00	tr	0.05 ± 0.01	0.14 ± 0.01
(13*Z*)-β-carotene	0.01 ± 0.00a	0.04 ± 0.00b	0.03 ± 0.00c	tr	tr	0.69 ± 0.02
(all-*E*)-α-carotene	tr	0.01 ± 0.00	0.01 ± 0.00	0.02 ± 0.00A	0.07 ± 0.01AB	0.44 ± 0.16B
(all-*E*)-β-carotene	0.35 ± 0.02a	0.78 ± 0.04b	0.56 ± 0.01c	1.05 ± 0.07A	4.25 ± 0.43B	6.74 ± 0.75C
(9*Z*)-β-carotene	0.02 ± 0.00a	0.03 ± 0.00b	0.03 ± 0.00c	0.15 ± 0.03A	0.69 ± 0.08B	1.44 ± 0.03C
Lutein ester 1	0.04 ± 0.00a	0.06 ± 0.00b	0.06 ± 0.00b	0.12 ± 0.07	tr	tr
Lutein dimyristate	0.02 ± 0.00a	0.03 ± 0.00b	0.01 ± 0.00c	0.07 ± 0.03A	0.60 ± 0.06B	0.95 ± 0.02C
Lutein ester 2	0.04 ± 0.00a	0.04 ± 0.00a	0.01 ± 0.00b	0.14 ± 0.09A	0.72 ± 0.02B	0.71 ± 0.05B
Lutein ester 3	0.04 ± 0.00a	0.03 ± 0.00b	0.01 ± 0.00c	0.16 ± 0.10A	0.81 ± 0.11B	0.95 ± 0.14B
Lutein 3-*O*-myristate-3′-*O*-palmitate	0.03 ± 0.00a	0.04 ± 0.01a	0.02 ± 0.00b	0.15 ± 0.07A	1.05 ± 0.01B	1.55 ± 0.17C
Lutein 3-*O*-palmitate-3′-*O*-myristate	0.03 ± 0.00a	0.03 ± 0.01a	0.01 ± 0.00a	0.16 ± 0.07A	0.95 ± 0.06B	1.26 ± 0.05C
Lutein dipalmitate	0.11 ± 0.00a	0.09 ± 0.00b	0.03 ± 0.00c	0.53 ± 0.26A	3.13 ± 0.06B	3.70 ± 0.65B
Total free carotenoids	0.49 ± 0.02a	1.00 ± 0.04b	0.78 ± 0.01c	3.39 ± 0.49A	6.40 ± 0.67B	11.23 ± 0.51C
Total carotenoid esters	0.32 ± 0.00a	0.32 ± 0.02a	0.15 ± 0.00b	1.32 ± 0.69A	7.26 ± 0.18B	9.11 ± 1.09B
Total carotenoids	0.81 ± 0.03a	1.32 ± 0.07b	0.93 ± 0.01a	4.71 ± 0.21A	13.65 ± 0.86B	20.34 ± 1.60C

RS ripening stage, *tr* not quantified trace amount (*S*/N < 10)

Data represent mean values ± standard deviation ($n = 2$), different lowercase letters within a row indicate significant differences of carotenoid contents in pulp of orange *Physalis* fruit ($P < 0.05$), different uppercase letters within a row indicate significant differences of carotenoid contents in peel of orange *Physalis* fruit ($P < 0.05$)

other chloroplast-specific carotenoids, e.g. (all-*E*)-violaxanthin and (all-*E*)-neoxanthin. (All-*E*)-α-carotene was exclusively detected in yellow (trace amounts) and orange (both 0.5%) *Physalis* fruit pulp and peel, while (all-*E*)-zeaxanthin was solely found in red *Physalis* fruit pulp and peel (1.2% and 2.2%, resp.).

In addition to non-esterified carotenoids, esters of carotenoids with fatty acids accumulated in all fruit at RS1 (5.8–67.3%). Yellow and orange *Physalis* fruit were characterized by lutein esters (Tables 1, 2), whereas red *Physalis* fruit exhibited a more diverse ester profile, including zeaxanthin, β-cryptoxanthin, lutein, antheraxanthin, mutatoxanthin, and violaxanthin esters (Table 3). Specifically, the ratio of carotenoid esters was found to be higher in pulp (23.8%, 39.3%, 67.3%) than in peel (5.8%, 27.7%, 53.3%) of yellow, orange and red *Physalis* fruit, respectively.

The color transition of all *Physalis* fruit from RS1 to RS2 was characterized by the massive decrease of lutein being the typical chloroplast carotenoid both in pulp and peel (Tables 1, 2, 3). However, the concomitant accumulation pattern of de novo appearing carotenoids differed among the three *Physalis* species. The coloration of yellow and orange *Physalis* was mainly contributed by β-carotene increasing to proportions of ca. 27–33% (yellow type) and 31–59% (orange type). Simultaneously, lutein esters were present at significant levels both at RS1 and RS2 (Tables 1, 2). In contrast to the relative β-carotene increase in yellow and orange *Physalis*, relative β-carotene levels even decreased in red *Physalis* fruit from 8.5 to 1.0% in pulp and from 11.3 to 0.6% in peel, while diverse carotenoid esters, e.g. zeaxanthin dipalmitate and β-cryptoxanthin palmitate, accumulated dramatically from 67.3 to 98.4% in pulp and from 53.3 to 96.7% in peel, respectively (Table 3). In terms of total carotenoid contents of different *Physalis* fruit at RS2, except for peel of yellow *Physalis* fruit, significant increases ($P < 0.05$) were observed as compared with those at RS1. A particularly striking 14- and 10-fold increase was found in pulp and peel of red *Physalis* fruit, respectively (Table 3).

At full ripeness (RS3), all *Physalis* fruit displayed their typical yellow, orange, and red color (Suppl. Figs. S1, S2, S3). Yellow and orange *Physalis* fruit presented similar carotenoid profiles in both pulp and peel at RS3. Predominant pigments were β-carotene (58.6–60.9%) and lutein esters (15.7–25.7%, Tables 1, 2), except for the peel of orange *Physalis* fruit, where a higher percentage of lutein esters (44.7%) and a lower proportion of β-carotene (33.1%) was observed. By contrast, red *P. alkekengi* fruit showed a qualitatively distinct carotenoid profile, in which carotenoid

Table 3 Carotenoid composition of red *Physalis* (*P. alkekengi*) fruit (meso- and exocarp) at different ripening stages

Compounds	Carotenoid content (mg/100 g FW)					
	Pulp			Peel		
	RS1	RS2	RS3	RS1	RS2	RS3
(all-*E*)-violaxanthin	tr	tr	tr	tr	tr	tr
(all-*E*)-neoxanthin	tr	tr	tr	tr	tr	tr
(all-*E*)-lutein	0.32 ± 0.01	tr	tr	3.49 ± 0.04A	0.60 ± 0.08B	0.06 ± 0.00C
(all-*E*)-zeaxanthin	0.02 ± 0.00a	0.06 ± 0.00b	0.06 ± 0.00c	0.23 ± 0.01A	0.67 ± 0.02B	0.64 ± 0.13B
(all-*E*)-β-cryptoxanthin	tr	0.04 ± 0.00	0.03 ± 0.00	tr	0.48 ± 0.03	0.36 ± 0.04
(13*Z*)-β-carotene	0.01 ± 0.00a	0.03 ± 0.00b	0.03 ± 0.00b	0.11 ± 0.03A	0.30 ± 0.06B	0.43 ± 0.04B
(all-*E*)-β-carotene	0.12 ± 0.01a	0.20 ± 0.02b	0.11 ± 0.00a	1.23 ± 0.08A	1.59 ± 0.04A	1.63 ± 0.28A
Lutein palmitate	tr	0.18 ± 0.01	0.11 ± 0.00	0.47 ± 0.02A	1.86 ± 0.02B	1.97 ± 0.31B
Zeaxanthin palmitate	0.02 ± 0.00a	0.67 ± 0.00b	1.54 ± 0.01c	0.11 ± 0.01A	2.71 ± 0.62A	12.65 ± 1.71B
Violaxanthin dipalmitate	tr	0.52 ± 0.06	0.54 ± 0.02	0.48 ± 0.06A	3.95 ± 1.17B	6.15 ± 0.31B
β-Cryptoxanthin palmitate isomer	tr	0.17 ± 0.01	0.13 ± 0.00	0.22 ± 0.01A	1.37 ± 0.22B	2.79 ± 0.26C
β-Cryptoxanthin palmitate	0.13 ± 0.00a	3.95 ± 0.00b	6.59 ± 0.03c	0.57 ± 0.03A	20.07 ± 3.60B	56.24 ± 4.48C
Antheraxanthin dipalmitate	tr	1.21 ± 0.09	0.76 ± 0.01	0.55 ± 0.06A	6.97 ± 2.60A	8.28 ± 2.11A
Zeaxanthin dimyristate	tr	0.11 ± 0.00	0.09 ± 0.01	0.15 ± 0.00A	0.61 ± 0.03B	0.74 ± 0.05B
Mutatoxanthin palmitoleate palmitate isomer	tr	0.07 ± 0.01	0.04 ± 0.01	0.18 ± 0.01A	0.59 ± 0.06B	0.43 ± 0.00C
Mutatoxanthin palmitoleate palmitate isomer	0.06 ± 0.00a	0.10 ± 0.00b	0.18 ± 0.00c	0.06 ± 0.01A	0.75 ± 0.19AB	1.41 ± 0.52B
Zeaxanthin palmitoleate palmitate	0.08 ± 0.01a	0.63 ± 0.00b	0.79 ± 0.01c	0.32 ± 0.02A	2.94 ± 0.02B	5.42 ± 0.26C
Zeaxanthin myristate palmitate + lutein dipalmitate	0.16 ± 0.00a	1.17 ± 0.00b	1.00 ± 0.01c	0.86 ± 0.02A	7.53 ± 0.46B	10.86 ± 0.89C
(13*Z*)-zeaxanthin dipalmitate	0.02 ± 0.00a	0.21 ± 0.01b	0.31 ± 0.04b	0.14 ± 0.04A	3.48 ± 0.52A	8.86 ± 1.54B
Zeaxanthin dipalmitate	0.49 ± 0.01a	11.20 ± 0.19b	14.98 ± 0.37c	1.56 ± 0.08A	51.00 ± 6.80B	138.01 ± 12.71C
(9*Z*)-zeaxanthin dipalmitate	0.01 ± 0.00a	0.07 ± 0.00b	0.11 ± 0.01c	0.11 ± 0.02A	1.11 ± 0.02B	2.55 ± 0.32C
Zeaxanthin palmitate stearate	tr	0.01 ± 0.00	0.03 ± 0.00	0.02 ± 0.00A	0.26 ± 0.01B	0.61 ± 0.06C
Total free carotenoids	0.47 ± 0.01a	0.34 ± 0.02b	0.23 ± 0.00c	5.07 ± 0.09A	3.63 ± 0.08B	3.12 ± 0.49B
Total carotenoid esters	0.97 ± 0.02a	20.29 ± 0.01b	27.20 ± 0.51c	5.79 ± 0.27A	105.21 ± 6.13B	256.95 ± 21.28C
Total carotenoids	1.44 ± 0.03a	20.62 ± 0.00b	27.43 ± 0.51c	10.86 ± 0.18A	108.84 ± 6.06B	260.07 ± 21.77C

RS ripening stage, *tr* not quantified trace amount (S/N < 10)

Data represent mean values ± standard deviation ($n = 2$), different lowercase letters within a row indicate significant differences of carotenoid contents in pulp of red *Physalis* fruit ($P < 0.05$), different uppercase letters within a row indicate significant differences of carotenoid contents in peel of red *Physalis* fruit ($P < 0.05$)

esters like zeaxanthin dipalmitate and β-cryptoxanthin palmitate represented approximately 99% of the total carotenoids (Table 3).

Development of chromoplasts of *Physalis* fruit during maturation

Upon inspection of sections of cells from the epidermis, three sub-epidermal layers, and inner pulp cells by light and transmission electron microscopy, the found chloro- and chromoplasts generally appeared highly similar irrespective of the pericarp cell layer in all studied *Physalis* fruits. Consistent with the emergence of colored fruit from green fruit (Suppl. Figs. S1, S2, S3), chromoplasts of yellow, orange, and red *Physalis* fruit developed from chloroplasts (Fig. 2a) with well-developed grana and stroma thylakoids, plastoglobules, and starch grains (Fig. 2b).

In yellow *Physalis* fruit, the green chloroplasts started to turn into yellow chromoplasts at RS2, still showing large starch grains as visualized by light microscopy (Fig. 3a). With progressing fruit ripening, starch grains gradually disappeared. At RS3, the appearance of the chromoplasts was more color-intense and characterized by an elongated shape (Fig. 3b). Furthermore, typical large, orange crystals were observed (Fig. 3c). According to our TEM graphs, grana thylakoids were disintegrated into single strands, and plastoglobules with increasing size accumulated at RS2 (Fig. 3d). In fully ripe yellow *Physalis* fruit, typical large carotene crystal remnants appeared in the chromoplasts. Only crystal remnants were visible, because the carotene crystals had been extracted during sample preparation. The former

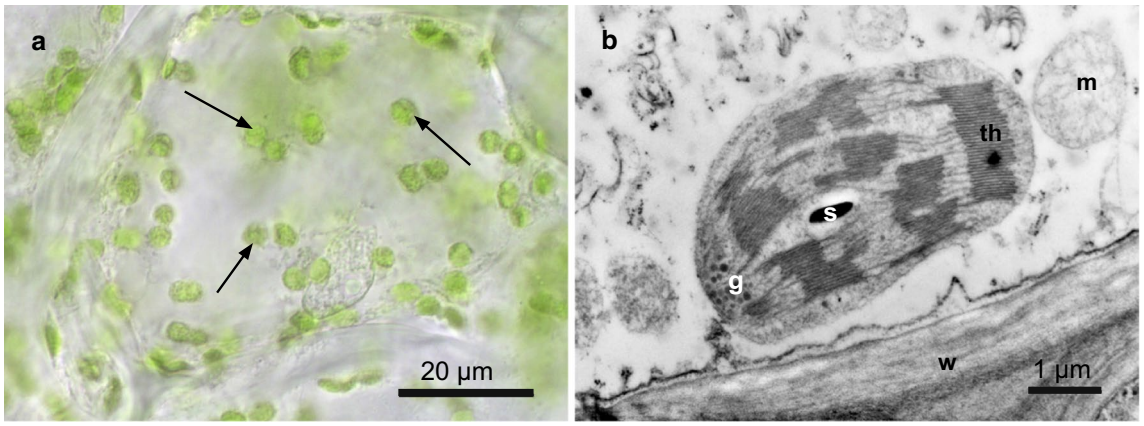

Fig. 2 Light micrograph (**a**) and TEM graph (**b**) of the green, unripe pericarp of *P. alkekengi* at RS1. **a** Chloroplasts (arrows) in an unripe pericarp cell (freehand section). **b** Chloroplast with numerous grana thylakoids (*th*), plastoglobules (*g*), and a starch grain (*s*). *m* mitochondrion, *w* cell wall

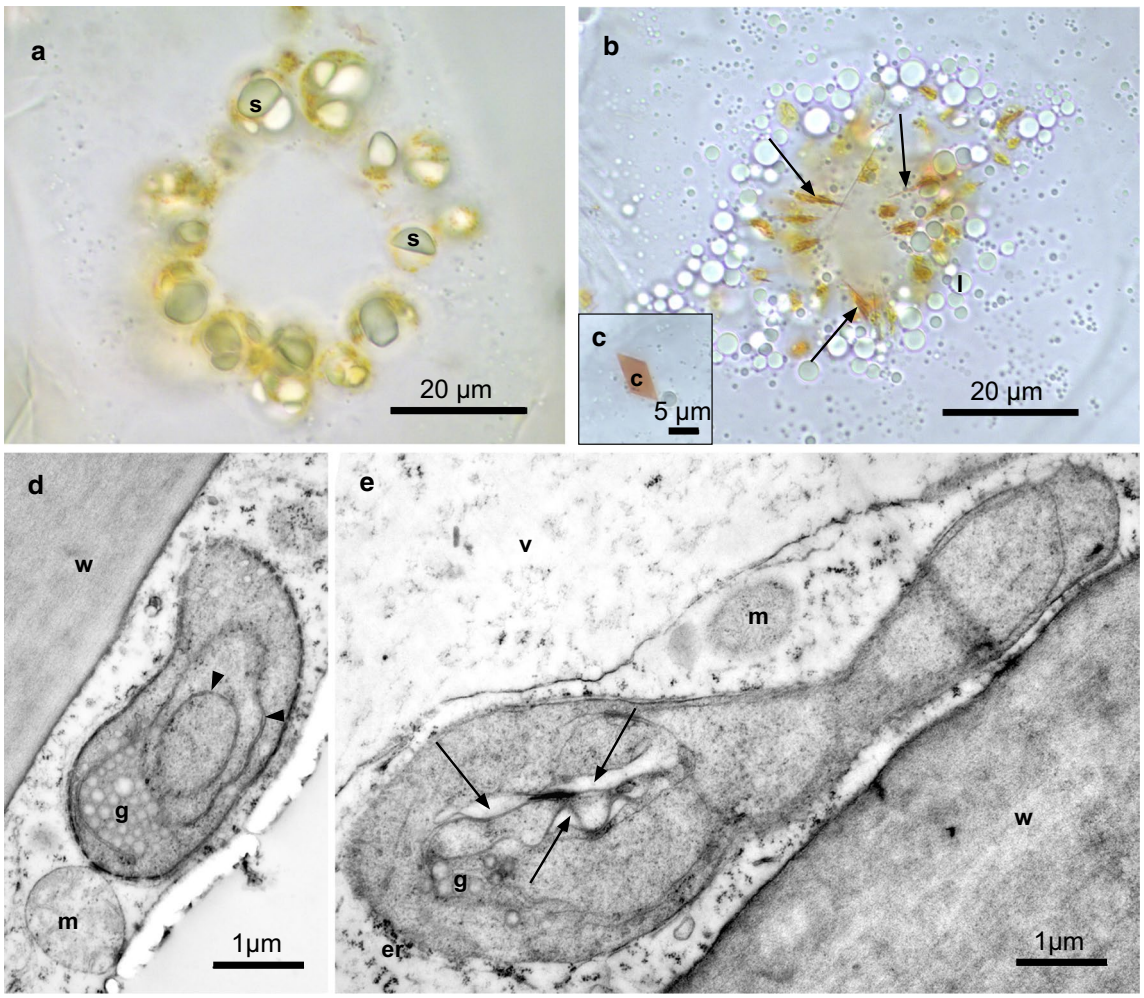

Fig. 3 Light micrographs (**a**–**c**) of freehand sections of the pericarp and TEM graphs (**d**, **e**) of chromoplasts of *P. pubescens*. **a** Developing chromoplasts at RS2 with large starch grains (*s*). **b** Chromoplasts at RS3. Chromoplasts with long crystals (arrows). *l* lipid bodies. **c** Detail of a plate-shaped crystal (*c*). **d** Chromoplast at RS2 with globules (*g*) and some stroma thylakoids (arrowheads). *m* mitochondrion, *w* cell wall. **e** Chromoplast at RS3 with globules (*g*) and crystal remnants with internal undulated membranes (arrows). *m* mitochondrion, *v* vacuole, *er* endoplasmic reticulum, *w* cell wall

crystal-surrounding membranes were clearly detectable as undulated internal structures (Fig. 3e).

In orange *Physalis* fruit, chromoplasts changed their round form to long, spindle-shaped form during their development (cf. Fig. 4a, c). At RS2, protruding filaments (Fig. 4a) and small crystals (Fig. 4b) had already been observed by light microscopy. Lugol's iodine solution was applied to highlight the size and form of the starch

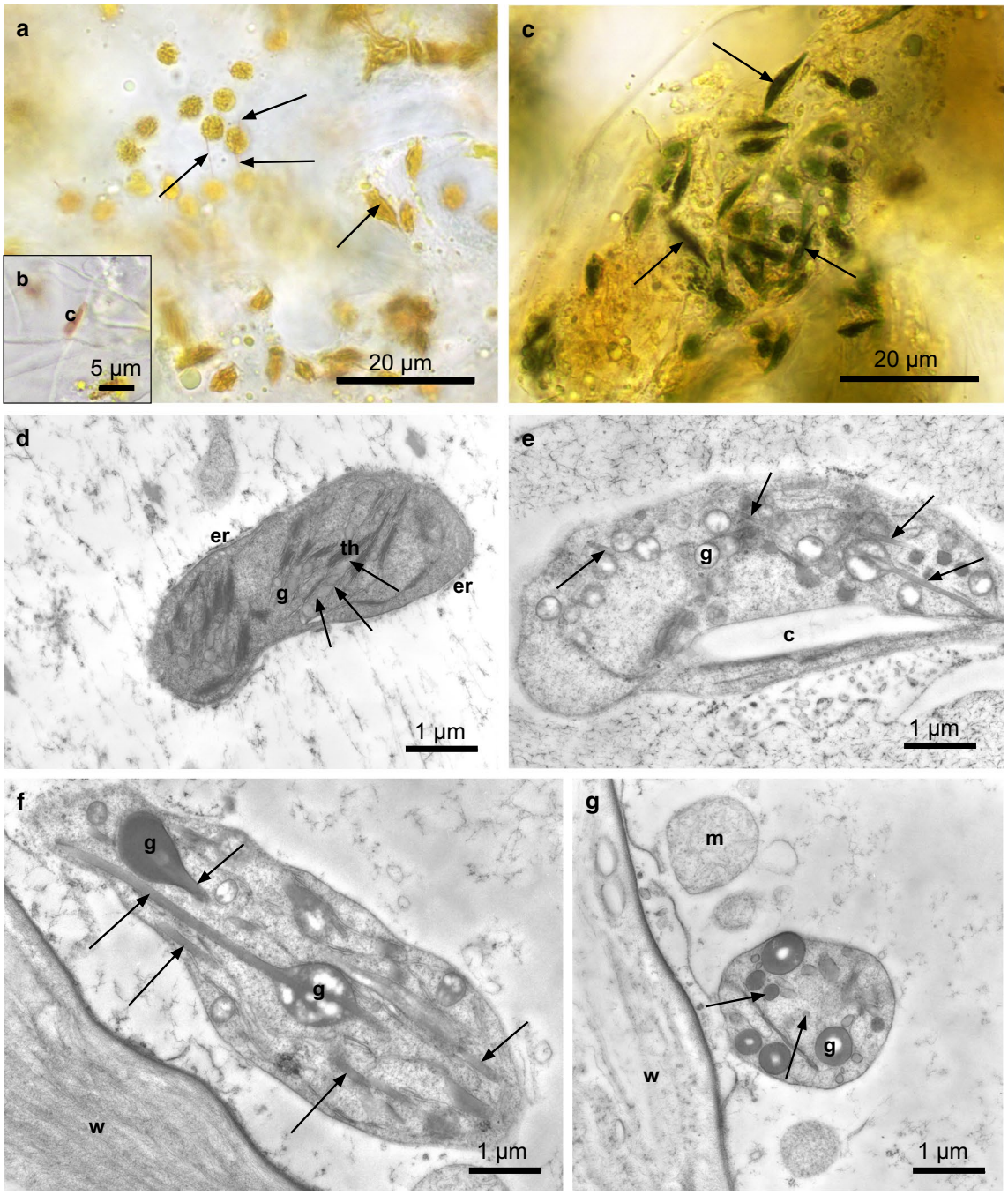

Fig. 4 Light micrographs (**a**–**c**) of freehand sections of the pericarp and TEM graphs (**d**–**g**) of chromoplasts of *P. peruviana*. **a** Chromoplasts at RS3 with long protruding filaments (arrows). **b** Inlay: rare crystal (*c*). **c** Chromoplasts at RS3. The spindle-shaped chromoplasts (arrows) after staining by Lugol's iodine solution. **d** Developing chromoplast at RS2 with grana thylakoids (*th*) and numerous globules (*g*). Some globules are elongated (arrows). Close contact of endoplasmic reticulum (*er*) to the envelope of the chromoplast. **e** Chromoplast at RS3 with crystal remnant (*c*), globules (*g*), and filaments (arrows). **f** Chromoplast at RS3, longitudinal-sectional view of filaments (arrows) in contact with globules (*g*). *w* cell wall. **g** Chromoplast at RS3, cross-sectional view of filaments (arrows) and globules (*g*). *m* mitochondrion, *w* cell wall

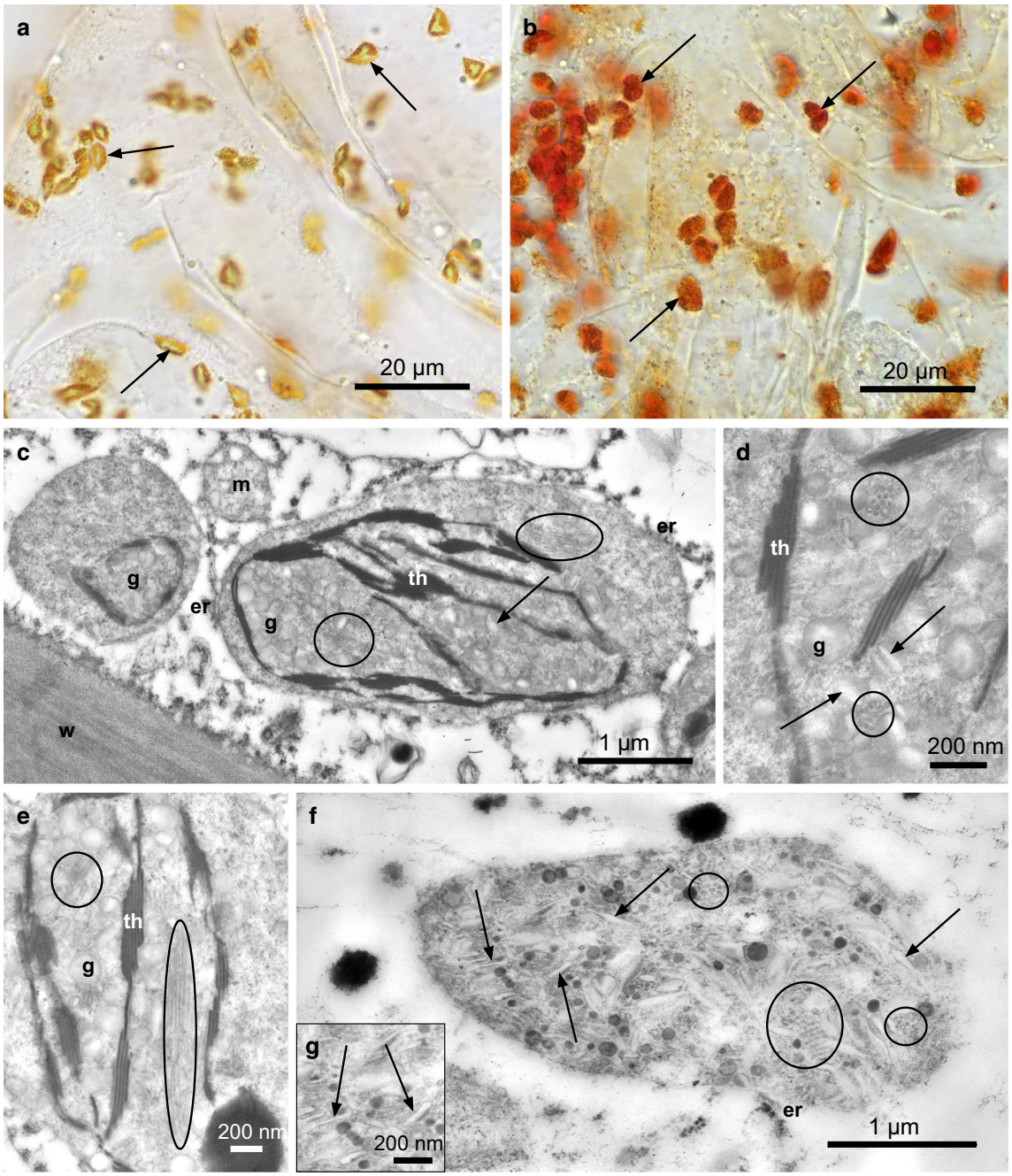

Fig. 5 Light micrographs (**a**, **b**) of freehand sections of the pericarp and TEM graphs (**c**–**g**) of chromoplasts of *P. alkekengi*. **a** Orange-green chromoplasts (arrows) at RS2. **b** Red chromoplasts (arrows) at RS3. **c** Chromoplasts at RS2 with developing tubule bundles (circles) and disc-like crystallites (arrow), as well as globules (*g*). Endoplasmic reticulum (*er*) close to the envelope. *m* mitochondrion, *th* thylakoids, *w* cell wall. **d** Detail of a chromoplast at RS2 with cross sectioned tubule bundles (circles) and developing disc-like crystallites (arrows). *g* globules, *th* thylakoids. **e** Detail of a chromoplast at RS2 with longitudinal sectioned tubule bundles (circles). *g* globules, *th* thylakoids. **f** Chromoplast at RS3 with accumulated tubule bundles (circles) and disc-like crystallites (arrows). Endoplasmic reticulum (*er*) close to the envelope. **g** Inlay: Detail of disc-like crystallites (arrows)

granules within the chromoplasts (Fig. 4c). Using TEM, at RS2, thylakoids were still obvious, while numerous plastoglobules accumulated (Fig. 4d). From these often large globules, thick and homogenously electron-dense filaments protruded frequently (Fig. 4d–f). Endoplasmic reticulum in close contact to the chromoplast envelope was conspicuous (Fig. 4d). At RS3, the aforementioned filaments became predominant elements (Fig. 4f, g). Moreover, crystal remnants surrounded by membranes were detected by TEM (Fig. 4e).

In red *Physalis* fruit, color changed from green to orange and finally to reddish orange. Their chromoplasts were round or oval-shaped (Fig. 5a,b), rather than elongated or spindle-shaped as described for yellow and orange *Physalis* fruit. As observed by light microscopy, the chloroplast-chromoplast transition along the envelope was ahead of that in the center of chromoplasts, where greenish areas were still visible at RS2 (Fig. 5a). In agreement, TEM graphs revealed grana thylakoids to be still present at RS2, although plastoglobules, tubule bundles and disc-like crystallites also clearly started to accumulate (Fig. 5c–e). In fully ripe red *Physalis* fruit, chromoplasts were filled with such apparently disc-like crystallites as well as bundles of tubules and plastoglobules (Fig. 5f, g).

Discussion

Carotenoid pattern and color of *Physalis* fruits

Fruit pulp and peel of all three *Physalis* species contained chloroplast-specific carotenoids at the early ripening stage (RS1), including β-carotene, lutein, and trace amounts of violaxanthin and neoxanthin, being consistent with carotenoid-rich fruit with initially green color such as tomato (Fraser et al. 1994). Meanwhile, the co-occurrence of xanthophyll esters indicated that the ripening-dependent carotenogenesis had just commenced at RS1 (Breithaupt and Schwack 2000; Rodriguez-Amaya 2001). With advancing ripeness, remarkable changes in carotenoid profiles occurred, resulting in total carotenoid contents being in agreement with those of earlier observations on whole fully ripe fruit (Weller and Breithaupt 2003; Deineka et al. 2008; Singh et al. 2012; Bravo et al. 2015; Wen et al. 2017; Etzbach et al. 2018).

As qualitative profiles of yellow (*P. pubescens*) and orange (*P. peruviana*) *Physalis* fruit were similar (Tables 1, 2), we suggest that the more intense, orange color of *P. peruviana* fruit was conveyed by their ca. 2–3 fold higher carotenoid contents (0.93 mg/100 g FW in pulp and 20.34 mg/100 g FW in peel) as compared to the paler yellow color of *P. pubescens* fruit (0.41 mg/100 g FW in pulp and 6.66 mg/100 g FW in peel). Besides increased absolute levels of lutein esters, also increased β-carotene concentrations might have particularly contributed to the observed color differences (cf. Tables 1, 2). In contrast, the qualitatively distinct carotenoid profile comprising mainly carotenoid esters (> 98%), and the strikingly high concentration of total carotenoids in red *Physalis* fruit, i.e., 27.43 mg/100 g FW in pulp and 260.07 mg/100 g FW in peel, strongly endowed them with the reddish orange tone. The distinct carotenoid profile of red *Physalis* (*P. alkekengi*) in contrast to yellow (*P. pubescens*) and orange (*P. peruviana*) *Physalis* concurred with their phylogenic relationship. Within the same genus, red *Physalis* belonged to the subgenus of *Physalis*, whereas yellow and orange *Physalis* were in the subgenus of *Rydbergis* although being grouped into different sections, i.e. *Epeteiorhiza* and *Lanceolatae*, respectively (Whitson and Manos 2005; Feng et al. 2016).

Carotenoid accumulation and chromoplast development

Chromoplasts are photosynthetically inactive plastids acting as metabolic sink of carotenoid biosynthesis to allow the massive accumulation of pigments imparting bright red, orange, and yellow hues to flowers, fruits, and vegetables (Sitte et al. 1980; Li and Yuan 2013; Schweiggert and Carle 2017). Chromoplasts often differentiate from chloroplasts during ripening of green unripe plant tissues or from non-green proplastids, leucoplasts or amyloplasts during ripening of white tissues (Li and Yuan 2013). In this study, chromoplasts of fruit from all three *Physalis* species were derived from chloroplasts according to our observations and in agreement with the ripening of initially green fruit. However, diverse carotenoid-bearing fine structural elements, such as plastoglobules, tubules, filaments, crystals, and disc-like crystallites, were found in chromoplasts of different colored *Physalis* fruit (Figs. 3, 4, 5), which were closely related to their distinct carotenoid profiles.

Plastoglobules have previously been demonstrated to be potential final storage sites of various carotenoids in different plants, such as of β-carotene in both mango (Vásquez-Caicedo et al. 2006) and peach palm fruit (Hempel et al. 2014), of lycopene (*Z*)-isomers in tangerine tomato (Cooperstone et al. 2015), and of xanthophylls and xanthophyll esters in yellow kiwi fruit (Montefiori et al. 2009), *Citrus* fruit (Lado et al. 2015; Lu et al. 2019), *Chrysanthemum* × *morifolium* flower (Huang et al. 2019), and tomato flower (Ariizumi et al. 2014). However, in most cases, plastoglobules are not the exclusive site of carotenoid deposition in chromoplasts. With progressive accumulation of carotenoids surpassing saturation concentration in plastoglobular lipids, excess carotenoids tend to aggregate and finally be deposited in crystalline form as solid crystals or in liquid-crystalline form in tubular structures (Deruère et al. 1994; Nogueira et al. 2013; Berry et al. 2019). This was confirmed by the present study where crystals, tubules, filaments, and a further unusual structure, presumably disc-like crystallites, appeared with increasing carotenoid contents, often being clearly associated with plastoglobules (Figs. 4e, f, 5d). Deposition of excess carotenoids in crystalline or liquid-crystalline state would presumably make them metabolically inert, osmotically immobile, and less prone to oxidative degradation than in the lipid-dissolved (in plastoglobules) state, concurrently thus avoiding possible toxic effects of overaccumulation of

lipoidal components on plastidal functions (Deruère et al. 1994; Nogueira et al. 2013).

Although requiring further study, β-carotene might be the major component of the typical crystals found in chromoplasts of fully ripe yellow and orange *Physalis* fruit, since the simultaneous emergence of these crystals and the increase in total carotenoid content from RS2 to RS3 in yellow *Physalis* fruit was highly associated to β-carotene accumulation (Table 1). In agreement, crystals have earlier been observed in plant tissues with high content in carotenes, i.e., pure hydrocarbon carotenoids, such as β-carotene-rich tissues like orange carrot roots (Steffen and Reck 1964; Kim et al. 2010), high-beta tomato mutant (Harris and Spurr 1969), sweet potato (Purcell et al. 1969; Jeffery et al. 2012), and the cauliflower *Or* mutant (Paolillo et al. 2004). Besides β-carotene, lycopene was also frequently found deposited as large crystals in fruits and vegetables, such as red tomato, red-fleshed watermelon, red grapefruit, Cara Cara oranges, red-fleshed papaya, and pink guava (Rojas-Garbanzo et al. 2017; Schweiggert and Carle 2017). The chromoplasts in the yellow fruit of *P. pubescens* may thus be classified as crystalloid chromoplasts.

Besides crystals, the chromoplasts of orange *Physalis* contained two other typical chromoplastidal elements (globules, filaments) at the same time, rendering an unambiguous chromoplast classification intricate. A similar type of chromoplast has been observed previously in red papaya fruit, where our group had hypothesized earlier that carotenoid esters were associated with the formation of "globule-associated tubules" and lycopene with crystal formation (Schweiggert et al. 2011a). We now believe that these "globule-associated tubules" would be better classified as "filaments" to allow distinguishing them from the below-mentioned "tubules" with a quite different appearance, i.e., the latter being very often observed in large bundles. While pure hydrocarbons like lycopene and β-carotene have been frequently found to be associated with the appearance of crystals, carotenoid esters were hypothesized to foster the self-assembly of tubular elements, which might have been denoted "filaments" in some cases as described above (Hempel et al. 2016; Schweiggert and Carle 2017). Thus, in orange *Physalis*, crystals and filaments might be speculated to comprise favorably β-carotene and lutein esters, respectively, although this hypothesis clearly requires further study. Similar types of filaments protruding from plastoglobules and often also ambiguously called "tubules" have been observed in other fruit concomitant with carotenoid accumulation, specifically xanthophyll esters, such as in red berries of *Palisota barteri* Hook. (Knoth et al. 1986), some orange cultivars of *Capsicum* fruit (Simpson et al. 1977), squash (Ljubešić 1977), fruit of *Solanum capsicastrum* Link. (Ljubešić et al. 2001), rose hips (Sitte et al. 1980), mango (Vásquez-Caicedo et al. 2006), red- and yellow-fleshed papaya (Schweiggert et al. 2011a), and red-fleshed loquat fruit (Fu et al. 2012).

In red fruit (*P. alkekengi*), the massive occurrence of an unusual type of chromoplastidal element was observed (Fig. 5d–g, arrows). It was clearly not formed by the nearly absent β-carotene (< 1% of total carotenoids in pulp at RS3), but possibly rather by the contained carotenoid esters (> 98%). We propose these elements to represent very small, possibly platelet-shaped or disc-like crystalline elements. Providing credit to their small size, Sitte et al. (1980) earlier proposed the name "crystallites" for this type of element. In contrast, typical chromoplast tubules are regularly shaped and thinner than these presumable platelet- or disc-like elements found in red *Physalis* fruit. Simpson et al. (1978) have earlier described these unusual substructures as "electron-transparent crystalloids" in red *Physalis* chromoplasts. They proposed zeaxanthin dipalmitate to be the main carotenoid deposited within these elements. Our study supports these findings, since it accounted for about half of the total carotenoid in red *Physalis* fruit (Table 3). However, zeaxanthin dipalmitate was earlier suggested to enable liquid-crystalline deposits within typical and highly regular chromoplast tubules of goji berries (*Lycium barbarum* L.), where it constituted more than 85% of total carotenoids (Hempel et al. 2017). The self-assembly hypothesis of carotenoid esters into these tubular forms has been supported by in vitro-aggregation of zeaxanthin dipalmitate as loosely packed J-aggregates forming potential nematic liquid crystals (Hempel et al. 2016). Disc-like elements similar to those described in our study were further observed in fruit of *Solanum pseudocapsicum* L., although being more likely formed by excess accumulation of β-carotene, which accounted for 85.5% of the total carotenoids (Simpson et al. 1978). In addition, gac fruit (*Momordica cochinchinensis* [Lour.] Spreng.), containing extremely high concentrations of lycopene (164 mg/100 g FW), showed no light microscopically visible crystals in chromoplasts, and it was speculated to deposit the substantial lycopene in very small crystallites as well (Müller-Maatsch et al. 2017), although TEM graphs are lacking to date. In brief, the development of chromoplastidal elements as observed in red *Physalis* fruit and the aforementioned fruit is not fully understood and merits further investigation.

Regarding typical chromoplast tubules, they were observed in red fruit and were mostly highly organized as tubule bundles (Fig. 5c–f, circles). In contrast to the single, thicker filaments of orange *Physalis* chromoplasts, the tubule bundles observed in red *Physalis* chromoplasts were organized in parallel and the single tubule had smaller diameter than the aforementioned filaments. Such tubules and tubule bundles have also been observed in many flowers like nasturtium petals (Sitte et al. 1980), and several fruits such as mango (Vásquez-Caicedo et al. 2006), goji berries (Hempel

et al. 2017), mamey sapote and red bell pepper (Chacón-Ordóñez et al. 2016). Since xanthophyll esters comprised 99% of total carotenoids in red *Physalis* fruit (Table 3), the tubule bundles were hypothesized to contain such xanthophyll esters. However, it is hard to identify the specific types of xanthophyll esters preferably stored in the tubule bundles, which still requires further chemical analyses on the separated structural elements, i.e., particularly on the tubule bundles, the filaments and the disc-like crystallites of *Physalis* chromoplasts, all three being believed to contain xanthophyll esters, possibly at different proportions. The mechanisms driving the formation of tubule bundles, filaments, and disc-like crystallites need to be elucidated in the future. Besides the lack of such fundamental insights, the impact of these three different deposition forms on stability and bioavailability of xanthophyll esters is unclear and merits further study.

Author contributions statement XW, AH, YN, RC, and RS conceived and designed the research. XW, AH, KW, and QH conducted the experiments. XW analyzed the data. XW and AH prepared the tables and figures. XW wrote the manuscript. All authors read, revised and approved the final manuscript.

Acknowledgements We thank Ms Johanna Ruhnau, master gardener, Botanical Garden, University of Hohenheim, for cultivation of *Physalis* plants and Ms Erika Rücker, Institute of Botany, University of Hohenheim, for technical assistance in TEM. This work was partially funded by China Postdoctoral Science Foundation (2019M650899). One of the authors (X.W.) gratefully acknowledges a scholarship from China Scholarship Council (CSC, Grant 201606350121).

Compliance with ethical standards

Conflict of interest The authors declare that they have no conflict of interest.

References

Ariizumi T, Kishimoto S, Kakami R et al (2014) Identification of the carotenoid modifying gene *PALE YELLOW PETAL 1* as an essential factor in xanthophyll esterification and yellow flower pigmentation in tomato (*Solanum lycopersicum*). Plant J 79:453–465

Bernstein PS, Li B, Vachali PP et al (2016) Lutein, zeaxanthin, and *meso*-zeaxanthin: the basic and clinical science underlying carotenoid-based nutritional interventions against ocular disease. Prog Retin Eye Res 50:34–66

Berry HM, Rickett DV, Baxter CJ et al (2019) Carotenoid biosynthesis and sequestration in red chilli pepper fruit and its impact on colour intensity traits. J Exp Bot 70:2637–2650

Bravo K, Sepulveda-Ortega S, Lara-Guzman O et al (2015) Influence of cultivar and ripening time on bioactive compounds and antioxidant properties in Cape gooseberry (*Physalis peruviana* L.). J Sci Food Agric 95:1562–1569

Breithaupt DE, Schwack W (2000) Determination of free and bound carotenoids in paprika (*Capsicum annuum* L.) by LC/MS. Eur Food Res Technol 211:52–55

Breithaupt DE, Wirt U, Bamedi A (2002) Differentiation between lutein monoester regioisomers and detection of lutein diesters from marigold flowers (*Tagetes erecta* L.) and several fruits by liquid chromatography-mass spectrometry. J Agric Food Chem 50:66–70

Britton G (1995) UV/visible spectroscopy. In: Britton G, Liaaen-Jensen S, Pfander H (eds) Carotenoids. Spectroscopy, vol 1B. Birkhäuser Verlag, Basel, Boston, Berlin, pp 13–62

Chacón-Ordóñez T, Esquivel P, Jiménez VM et al (2016) Deposition form and bioaccessibility of keto-carotenoids from mamey sapote (*Pouteria sapota*), red bell pepper (*Capsicum annuum*), and sockeye salmon (*Oncorhynchus nerka*) filet. J Agric Food Chem 64:1989–1998

Chacón-Ordóñez T, Schweiggert RM, Bosy-Westphal A et al (2017) Carotenoids and carotenoid esters of orange- and yellow-fleshed mamey sapote (*Pouteria sapota* (Jacq.) H.E. Moore & Stearn) fruit and their post-prandial absorption in humans. Food Chem 221:673–682

Cooperstone JL, Ralston RA, Riedl KM et al (2015) Enhanced bioavailability of lycopene when consumed as *cis*-isomers from *tangerine* compared to red tomato juice, a randomized, cross-over clinical trial. Mol Nutr Food Res 59:658–669

Deineka VI, Sorokopudov VN, Deineka LA et al (2008) Studies of *Physalis alkekengi* L. fruits as a source of xanthophylls. Pharm Chem J 42:87–88

Delgado-Pelayo R, Gallardo-Guerrero L, Hornero-Méndez D (2014) Chlorophyll and carotenoid pigments in the peel and flesh of commercial apple fruit varieties. Food Res Int 65:272–281

Delgado-Pelayo R, Gallardo-Guerrero L, Hornero-Ménndez D (2016) Carotenoid composition of strawberry tree (*Arbutus unedo* L.) fruits. Food Chem 199:165–175

De Rosso VV, Mercadante AZ (2007) Identification and quantification of carotenoids, by HPLC-PDA-MS/MS, from amazonian fruits. J Agric Food Chem 55:5062–5072

Deruère J, Römer S, D'Harlingue A et al (1994) Fibril assembly and carotenoid overaccumulation in chromoplasts: a model for supramolecular lipoprotein structures. Plant Cell 6:119–133

Dugo P, Herrero M, Kumm T et al (2008) Comprehensive normal-phase × reversed-phase liquid chromatography coupled to photodiode array and mass spectrometry detection for the analysis of free carotenoids and carotenoid esters from mandarin. J Chromatogr A 1189:196–206

Etzbach L, Pfeiffer A, Weber F, Schieber A (2018) Characterization of carotenoid profiles in goldenberry (*Physalis peruviana* L.) fruits at various ripening stages and in different plant tissues by HPLC–DAD–APCI–MS^n. Food Chem 245:508–517

Facundo HVDV, Gurak PD, Mercadante AZ et al (2015) Storage at low temperature differentially affects the colour and carotenoid composition of two cultivars of banana. Food Chem 170:102–109

Feng S, Jiang M, Shi Y et al (2016) Application of the ribosomal DNA ITS2 region of *Physalis* (Solanaceae): DNA barcoding and phylogenetic study. Front Plant Sci 7:1047

Fraser PD, Truesdale MR, Bird CR et al (1994) Carotenoid biosynthesis during tomato fruit development. Plant Physiol 105:405–413

Fu X, Kong W, Peng G et al (2012) Plastid structure and carotenogenic gene expression in red-and white-fleshed loquat (*Eriobotrya japonica*) fruits. J Exp Bot 63:341–354

Grune T, Lietz G, Palou A et al (2285S) Beta-carotene is an important vitamin A source. J Nutr 140:2268S–2285S

Gupta P, Sreelakshmi Y, Sharma R (2015) A rapid and sensitive method for determination of carotenoids in plant tissues by high performance liquid chromatography. Plant Methods 11:5

Harris WM, Spurr AR (1969) Chromoplasts of tomato fruits. I. Ultrastructure of low-pigment and high-beta mutants. Carotene analyses. Am J Bot 56:369–379

Hempel J, Amrehn E, Quesada S et al (2014) Lipid-dissolved γ-carotene, β-carotene, and lycopene in globular chromoplasts of peach palm (*Bactris gasipaes* Kunth) fruits. Planta 240:1037–1050

Hempel J, Schädle CN, Leptihn S et al (2016) Structure related aggregation behavior of carotenoids and carotenoid esters. J Photochem Photobiol A Chem 317:161–174

Hempel J, Schädle CN, Sprenger J et al (2017) Ultrastructural deposition forms and bioaccessibility of carotenoids and carotenoid esters from goji berries (*Lycium barbarum* L.). Food Chem 218:525–533

Huang H, Lu C, Ma S et al (2019) Different colored *Chrysanthemum*×*morifolium* cultivars represent distinct plastid transformation and carotenoid deposit patterns. Protoplasma. https://doi.org/10.1007/s00709-019-01406-x

Jeffery J, Holzenburg A, King S (2012) Physical barriers to carotenoid bioaccessibility. Ultrastructure survey of chromoplast and cell wall morphology in nine carotenoid-containing fruits and vegetables. J Sci Food Agric 92:2594–2602

Johnson EJ (2014) Role of lutein and zeaxanthin in visual and cognitive function throughout the lifespan. Nutr Rev 72:605–612

Kilcrease J, Rodriguez-Uribe L, Richins RD et al (2015) Correlations of carotenoid content and transcript abundances for fibrillin and carotenogenic enzymes in *Capsicum annum* fruit pericarp. Plant Sci 232:57–66

Kim JE, Rensing KH, Douglas CJ, Cheng KM (2010) Chromoplasts ultrastructure and estimated carotene content in root secondary phloem of different carrot varieties. Planta 231:549–558

Knoth R, Hansmann P, Sitte P (1986) Chromoplasts of *Palisota barteri*, and the molecular structure of chromoplast tubules. Planta 168:167–174

Lado J, Zacarías L, Gurrea A et al (2015) Exploring the diversity in *Citrus* fruit colouration to decipher the relationship between plastid ultrastructure and carotenoid composition. Planta 242:645–661

Li L, Yuan H (2013) Chromoplast biogenesis and carotenoid accumulation. Arch Biochem Biophys 539:102–109

Ljubešić N (1977) The formation of chromoplasts in fruits of *Cucurbita maxima* Duch. '*turbaniformis*'. Bot Gaz 138:286–290

Ljubešić N, Wrischer M, Prebeg T, Brkić D (2001) Carotenoid-bearing structures in fruit chromoplasts of *Solanum capsicastrum* Link. Acta Bot Croat 60:131–139

Lu P, Wang S, Grierson D, Xu C (2019) Transcriptomic changes triggered by carotenoid biosynthesis inhibitors and role of *Citrus sinensis phosphate transporter 4;2* (*CsPHT4;2*) in enhancing carotenoid accumulation. Planta 249:257–270

Melendez-Martinez AJ, Stinco CM, Liu C, Wang XD (2013) A simple HPLC method for the comprehensive analysis of *cis/trans* (*Z*/*E*) geometrical isomers of carotenoids for nutritional studies. Food Chem 138:1341–1350

Mercadante AZ, Rodrigues DB, Petry FC, Mariutti LRB (2017) Carotenoid esters in foods—a review and practical directions on analysis and occurrence. Food Res Int 99:830–850

Montefiori M, McGhie TK, Hallett IC, Costa G (2009) Changes in pigments and plastid ultrastructure during ripening of green-fleshed and yellow-fleshed kiwifruit. Sci Hortic (Amsterdam) 119:377–387

Müller-Maatsch J, Sprenger J, Hempel J et al (2017) Carotenoids from gac fruit aril (*Momordica cochinchinensis* [Lour.] Spreng.) are more bioaccessible than those from carrot root and tomato fruit. Food Res Int 99:928–935

Nisar N, Li L, Lu S et al (2015) Carotenoid metabolism in plants. Mol Plant 8:68–82

Nogueira M, Mora L, Enfissi EMA et al (2013) Subchromoplast sequestration of carotenoids affects regulatory mechanisms in tomato lines expressing different carotenoid gene combinations. Plant Cell 25:4560–4579

Olivares-Tenorio M-L, Dekker M, Verkerk R, van Boekel MAJS (2016) Health-promoting compounds in cape gooseberry (*Physalis peruviana* L.): review from a supply chain perspective. Trends Food Sci Technol 57:83–92

Paolillo DJ, Garvin DF, Parthasarathy MV (2004) The chromoplasts of *Or* mutants of cauliflower (*Brassica oleracea* L. var. *botrytis*). Protoplasma 224:245–253

Petry FC, Mercadante AZ (2016) Composition by LC-MS/MS of new carotenoid esters in mango and citrus. J Agric Food Chem 64:8207–8224

Purcell AE, Walter WM, Thompkins WT (1969) Relationship of vegetable color to physical state of the carotenes. J Agric Food Chem 17:41–42

Rivera SM, Christou P, Canela-Garayoa R (2014) Identification of carotenoids using mass spectrometry. Mass Spectrom Rev 33:353–372

Rodriguez-Amaya DB (2001) A guide to carotenoid analysis in foods. ILSI Press, Washington

Rojas-Garbanzo C, Gleichenhagen M, Heller A et al (2017) Carotenoid profile, antioxidant capacity, and chromoplasts of pink guava (*Psidium guajava* L. cv. 'Criolla') during fruit ripening. J Agric Food Chem 65:3737–3747

Schweiggert RM, Carle R (2017) Carotenoid deposition in plant and animal foods and its impact on bioavailability. Crit Rev Food Sci Nutr 57:1807–1830

Schweiggert RM, Steingass CB, Heller A et al (2011a) Characterization of chromoplasts and carotenoids of red- and yellow-fleshed papaya (*Carica papaya* L.). Planta 234:1031–1044

Schweiggert RM, Steingass CB, Mora E et al (2011b) Carotenogenesis and physico-chemical characteristics during maturation of red fleshed papaya fruit (*Carica papaya* L.). Food Res Int 44:1373–1380

Schweiggert RM, Vargas E, Conrad J et al (2016) Carotenoids, carotenoid esters, and anthocyanins of yellow-, orange-, and red-peeled cashew apples (*Anacardium occidentale* L.). Food Chem 200:274–282

Simpson DJ, Baqar MR, Lee TH (1977) Chromoplast ultrastructure of *Capsicum* carotenoid mutants I. Ultrastructure and carotenoid composition of a new mutant. Zeitschrift für Pflanzenphysiologie 83:293–308

Simpson DJ, Baqar MR, Lee TH (1978) Chromoplast ultrastructure in fruit of *Solanum pseudocapsicum* and fruit and sepals of *Physalis alkekengi*. Aust J Bot 26:793–806

Singh DB, Pal AA, Lal S et al (2012) Growth and development changes of cape gooseberry (*Physalis peruviana* L.) fruits. Asian J Hortic 7:374–378

Sitte P, Falk H, Liedvogel B (1980) Chromoplasts. In: Czygan F (ed) Pigments in plants. Fisher, Stuttgart, pp 117–148

Steffen K, Reck G (1964) Chromoplastenstudien III. Die chromoplastengenese und das problem der plastidenhullen bei Daucus carota. Planta 60:627–648

Turcsi E, Nagy V, Deli J (2016) Study on the elution order of carotenoids on endcapped C18 and C30 reverse silica stationary phases. A review of the database. J Food Compos Anal 47:101–112

Van Breemen RB, Dong L, Pajkovic ND (2012) Atmospheric pressure chemical ionization tandem mass spectrometry of carotenoids. Int J Mass Spectrom 312:163–172

Vásquez-Caicedo AL, Heller A, Neidhart S, Carle R (2006) Chromoplast morphology and β-carotene accumulation during postharvest ripening of mango cv. "Tommy Atkins". J Agric Food Chem 54:5769–5776

Weller P, Breithaupt DE (2003) Identification and quantification of zeaxanthin esters in plants using liquid chromatography-mass spectrometry. J Agric Food Chem 51:7044–7049

Wen X, Hempel J, Schweiggert RM et al (2017) Carotenoids and carotenoid esters of red and yellow *Physalis* (*Physalis alkekengi* L. and *P. pubescens* L.) fruits and calyces. J Agric Food Chem 65:6140–6151

Wen X, Erşan S, Li M et al (2019) Physicochemical characteristics and phytochemical profiles of yellow and red *Physalis* (*Physalis alkekengi* L. and *P. pubescens* L.) fruits cultivated in China. Food Res Int 120:389–398

Whitson M, Manos PS (2005) Untangling *Physalis* (Solanaceae) from the Physaloids: a two-gene phylogeny of the Physalinae. Syst Bot 30:216–230

Zanatta CF, Mercadante AZ (2007) Carotenoid composition from the Brazilian tropical fruit camu-camu (*Myrciaria dubia*). Food Chem 101:1526–1532

Ziegler JU, Wahl S, Würschum T et al (2015) Lutein and lutein esters in whole grain flours made from 75 genotypes of 5 *Triticum* species grown at multiple sites. J Agric Food Chem 63:5061–5071